CHAPTER 2

Literature Reviews and Related Theories

The beginning of this chapter gives a short overview of CD4+ lymphocyte counting including cells staining and detection method. The previous studies on cell detection on bright field and fluorescence images are then reviewed separately since the study of cell detection on image fusion is rarely published.

2.1 CD4+ Lymphocyte Counting

2.1.1 Immunofluorescence for Cell Staining

Fluorescent dyes can be excited by light at the specific wavelength and emit a different wavelength depending on the type of dyes. Its electrons are arranged in discrete energy levels surrounding the atom's nucleus. Electrons in each level have a predetermined amount of energy. When the photon of light transmits the energy to electron, it becomes excited and jumps to a higher level of unstable of energy. The excited state takes a short duration. The electron loses a small energy as heat but the extra energy emits in the form of a photon when goes back to stable stage. Because the emitted fluorescence has a lower energy than the absorbed light so the wavelength of the emitted light is longer than excited light [2].

Immunofluorescence is a technique which has been widely used in scientific research and clinical diagnostics. This technique is based on the immunology knowledge; antigen-antibody reaction. Since the property of coupling specifically with their own antigens, antibodies are used as a tool for detecting the preferred target. Typically, antibodies are tagged with fluorescent dyes. So the binding element can be detected via the fluorescent dyes. The method of immunofluorescence staining is commonly divided into 2, i.e., direct and indirect staining, which are described in the Fig.2.1. The antibodies that bind against the target molecule are directly conjugated with the fluorescent dye for direct staining. In contrast, for indirect staining, the primary

antibodies that bind against the target molecule are untagged. Instead, fluorescent dyes are labeled to the anti-immunoglobulin antibodies called secondary antibody, which couple with the constant portion of the primary antibodies. The indirect staining method is claimed for the higher sensitivity since more than one secondary antibody can bind to one primary antibody. Finally, the complex can be detected using machine which equipped with fluorescence detection system.

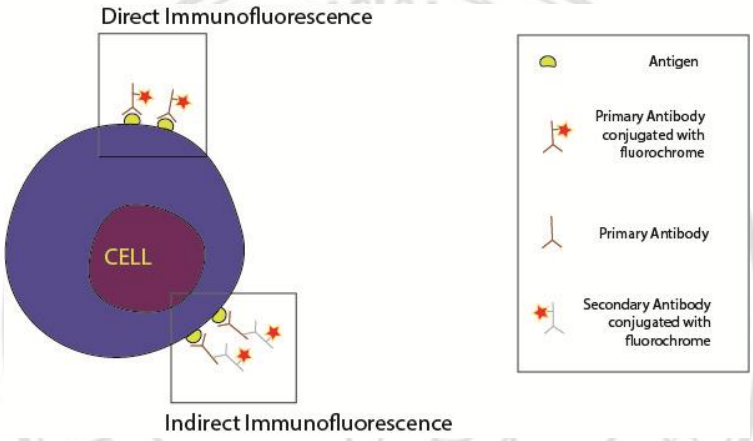

Figure 2.1 Schematic of direct and indirect immunofluorescence.

2.1.2 Methods for CD4+ Lymphocyte Counting

The standard method for CD4+ lymphocyte counting is flow cytometry. This instrument measures the physical and illumination of the cell or particle which single flows in the fluid stream through the light beam and thus, gives the individual information of detected object. The principle of this technique is based on the fact that cells or particles can be separated based on size, structure, granularity and component properties [3]. The instrument is divided into 3 main parts: fluidic system, optical system and detection system. Cells or particles must be suspended in the optimal solution then they are flowed via the fluidic stream. By the effect of sheath fluid system which faster flows surround the central core so called the hydrodynamic focusing, cells flow individually through the detection chamber. A laser beam hits a cell one at a time as they flow into the chamber. Light from a laser beam that strikes forward the cell and lays a shadow over the detector which measures the cell size is called Forward Scatter

(FSC). Meanwhile, light also dispersed into the wide angles when hits the internal irregular textures or granules and the scattered light can be detected by the Side Scatter (SSC) detector. Besides, the fluorescence information can be detected by the fluorescence detection system contained a specific wavelength mirror and filter and photomultiplier tube (PMT) [4]. Because of the broad function and effectiveness, flow cytometer has been widely used in many research fields and clinical diagnosis for more than two decades.

However, image-based cell detection methods were also invented and, several years ago, the automatic image-based CD4+ lymphocyte counting instrument is available in the market with brand, Alere Pima^{TM} CD4. CD4+ lymphocyte can be detected via bi-color fluorescence images captured under low magnification. The results obtained using the automatic image-based CD4+ cell counting system showed a high similarity to those obtained using flow cytometer. However, counting cells using only fluorescence images has certain limitations since nothing can prove that the color spots are actually cells. In this study, we solve this problem using the corresponding bright field image to guarantee the reliability of our fluorescence cell detection method.

2.1.3 Fluorescence Microscope

Fluorescence microscope has become an essential tool in research and clinical diagnosis. It is very useful for examining the structure and component of cells. It was developed from the light microscope by adding the fluorescence detection system. So, a fluorescence microscope contains two light sources: visible light generated lamp and ultraviolet (UV) lamp. Visible light generated lamp is the light source that also installed in the light microscope for bright field viewing. It gives the wavelength of visible light ranged between 380–700 nm. The viewing of fluorescence information uses UV produced by mercury, xenon lamp or sometimes laser. The microscope equips the set of specific wavelength mirror and filter. Light from the UV generated lamp hits the dichroic mirror which reflects the UV light to the specimen. The fluorescent substance absorbs the energy and emits the specific wavelength through the objective lens, passes the band-pass filter through the eyepiece and the image is generated [2].

2.2 Study of Image-Based Cell Detection and Counting

2.2.1 Cell Detection in Bright Field Images

The bright field is the simplest technique for cell morphology examination which acquires only a visible light. So that is the reason why using bright field image is the cheapest and effective way to prove that a color spot in the fluorescence image is truly a cell. The studies [5-10] detected cells in bright field images based on machine learning techniques.

T. Kazmar et al. [5], proposed the cell detection algorithm for phase contranst microscope of cancer cell based on the supervised method. Cell locations were identified by seed finding using the local intensity information. They used radial symmetry decomposition and blob-like key point to deal with the initial seeding step. Then, the Random forest (RF) algorithm was used to learn the outstanding 6 different features, i.e. nucleus, membrane, Halo, border, float and background of image partitioned by using 14 texture features. Then the partitioning result is used to consider which seeds belong to cells. Using the RF for classifying of image partition based on 6 different features gave a high precision though some features were hard to separate such as membrane from background and border from nucleus.

X. Long et al. [6], developed a patch-based cell recognition approach. The method was divided into preprocessing and classification step. Fisher Linear Discriminant (FLD) was used to reduce the dimension of feature vector of all patched images instead of a classical PCA. The 25x25 pixels of image patches were classified into 11 classes, i.e., cell and non-cell which contained more of 10 subclasses. This study used ANN for classification problem. The experiment was conducted on the both microsperes and living cells in bright field images. For microspheres, FLD showed a lower missed classification rate than PCA under these conditions; focus, illumination, size and noise. Likewise, FLD showed the high performance for cell recognition in three scenarios. Scenario1 showed a clean and completely separated cell. Scenario 2, debris and some clumping cells were present. Lastly, scenario 3 contained more high aggregated cells.

F. Mualla et al. [7], generated the automatic cell detection on cell line image. Scaled-Invariant Feature Transform (SIFT) was used to define cell and non-cell keypoints on the defocused cells image. Balance Random Forest (BRF) was employed to classify whether keypoints are cells or non-cells using keypoint profile in order to deal with the imbalance sample size. Then, obtained keypoints of cells were classified into inner and cross profile based on profile features. Then the graph-based approach is used for grouping the linkage keypoints which contained the similar information. The results of the experiment on sf21 cells (insect cell) detection whose characteristics are similar to WBCs in our study showed a high percentage of recall and precision but the segmentation results were not mentioned.

M. Tscherepanow et al. [8], proposed the automatic method for sf9 cell detection in bright field images instead of the conventional detection using fluorescence images since the cell information is more outstanding. The gray top-hat transform was used to separate the area of cells from background, resulting in a background image. In parallel, opening operator with the different orientation were applied repeatedly to find the cell membrane and the result images were fused together by computing point-wise maximum. Then cell markers were indicated by finding the point whose distance from the background and cell membrane is the longest. The 3 mentioned images were used as the parameter of snake algorithm for cell segmentation. The obtained segmentation showed an accurate contour. Another study of the same authors [9] presented the cell classification approach after segmentation. Correlation Analysis (CA) and PCA were used to reduce the features of data set. Then, classification was performed by SFAM and SVM. All classification techniques demonstrated better results than manual detection.

2.2.2 Cell Detection in Fluorescence Images

Cell detection in fluorescence image is very popular topic on biological and medical application. I. Smal et al. [10], studied on various comparative detection methods for detecting spots in fluorescence image. The detection frame work was commonly divided into 3 main steps. Noise reduction, signal enhancement and signal thresholding. Most cases used the Gaussian or matched filtering to increase SNR. For signal enhancement, both supervised and unsupervised approaches were stated. For

unsupervised based technique, they described several techniques, i.e., wavelet multiscale product, multiscale variance-stabilizing transform detector, top-hat filtering, Spot enhance filtering, gray opening top-hat transform, H-dome and some features based detection. For the supervised method, Adaboost and Fisher Discriminant Analysis (FDA) were explained. The result showed that supervised techniques gave a better performance than those unsupervised techniques. However, the results of the unsupervised technique such as multi-scale variance-stabilizing transform (MVST) and H-minima transform were also preferred. Basically, images taken by fluorescence imaging have a low resolution, resulting in diffraction-limited appearance. Hence, the detection based on unsupervised method, will be more effective if the images were appropriately pre-treated.

There are many techniques for image pre-processing depending on the appearance of the image. E. Alban et al. [11], proposed the local enhancement of cells in confocal microscopic images based on the intensity profile in RGB using statistical parameters such as mean and variance.

Besides, the intensities of uneven background can be corrected by subtracting with the background estimation function [12, 13]. T. Pecot et al. [12], studied on the vesicle segmentation within cytosol in live cell imaging. The proposed method named C-CRAFT, used the conditional random field to represent the image information. In this study, background estimation was done to improve the detection of vesicle whose intensity is the additive signal from fluorescence signal of the background. The statistical Bayesian approach was applied to separate the points which belong to the background from the vesicle in the conditional random field. Since the objective of this study is to segment the moving vesicles in live cell imaging, the information of all sequences were used together for background estimation simultaneously with vesicle segmentation. The result of this study show a better performance for the real fluoresence image than the others.

C. Wählby et al. [13], proposed the algorithm for segmentating cytoplasm of the fluorescence labelled cells. Because of uneven illumination of the background, the pre-processing step was performed. The 5x5 evenly spread control points of B-spline function was used to estimate the shading of the background. The background

estimation was done iteratively in order to generate more accurate background fitting. The B-spline function was applied to the whole image for initializing the estimation then background compensate image was obtained from the subtraction of original image and first background estimation. After computing standard diviation (SD) of background compensate image, pixels whose SD values are higher than constant value were assigned as foreground. The next iterative was done continuously on the original image where the foreground pixels have been already discarded until the average change of the obtained estimated background was less than a half of quantization of original image. The image after pre-processing which determined by visualization was well improved.

After preprocessing steps, the segmentation technique will be applied. Thresholding is the simplest technique for this task [14]. However, more difficult problems require more complicated technique to deal with, such as a watershed algorithm [13,15,16], graph cuts [18], and clustering algorithm [19].

2.2.3 Cell Detection in Image Fusion

The study on cell detection based on different types of image is rarely published. The reviewed study is very similar to our work since the yeast cells were detected based on bright field, green fluorescence and red fluorescence images [14] based on the simple thresholding.

A. Korzyńska et al. [20], developed the segmentation algorithm using both bright field and fluorescence images. The texture-based method was applied to bright field image in order to identify the cell markers based on the position, shape and texture information. Then the segmentation was refined in fluorescence image by applying morphological operation and thresholding. Similar to the study on yeast detection [21], the bright field image was used to address the cell location prior to determine the specific gene containing in fluorescence image.

Our research involves cell detection in bright field image, fluorescence image and image fusion. The white blood cells in bright field image are detected. Then, positive cell in green and red fluorescence image are also detected. Finally, detected regions among three images are then combined in order to find the overlapping area and thus,

counting the overlapping area. The overall algorithms will be performed based on the unsupervised method since we want to avoid the complication on appropriate sample selection for a good training system.

2.3 Fundamental Theories Used in This Study

This section describes the theories used in this study. Basically, we develop the algorithm based on the unsupervised method.

2.3.1 Image Conversion

The color space used in this study basically is RGB. In the segmentation using multi-gray scale image (chapter 3; section 3.1.2), we use gray scale and R channel images. The chrominance image converted from RGB can be calculated by

$$f_{chroma} = 0.211R - 0.523G + 0.312B \quad (1)$$

2.3.2 Canny Edge Detection

The performance of the canny approach is based on 3 criterions; good edge detection, well edge localization and single edge point response [22]. The method consists of 4 main steps as described below

Step 1: Noise reduction

Canny algorithm assumes the edge and additive white Gaussian noise exists in the image. So, the Gaussian filter is used to reduce the noise and occasionally reveal the truth edges.

Step 2: Gradient magnitude and direction computation

The edge is connected pixels where the meaningful transition of the intensity on the image located. The transition of intensity or gradient can be calculated by using the discrete derivation of image. In Canny method, the magnitude and direction of gradient on the image can be calculated by convolution of an image with the Sobel operator (Fig. 2.2). The magnitude and direction of the gradient can be obtained by (2) and (3) respectively.

$$|G| = \sqrt{G_x^2 + G_y^2} \tag{2}$$

$$\theta(x, y) = \tan^{-1}\left(\frac{G_y}{G_x}\right) \tag{3}$$

where G_x and G_y are the gradient image along the x and y directions.

Step 3: Non-maximum suppression

According to the concept that truth edges have higher gradient, non-maximum suppression tends to generate the thin truth edge by finding the maximum magnitude among the neighborhoods along the gradient direction.

Step 4: Double thresholding and edge hysteresis

The edge hysteresis is used to eliminate streaking which is the breaking of an edge. The two thresholding values are applied. Any pixel on the image that has a value greater than T1 is assumed to be an edge. Then, any pixel which connects to these edge pixels whose value greater than T2 is also assigned as edge pixels.

1	2	1
0	0	0
-1	-2	-1

G_x

1	0	-1
2	0	-2
1	0	-1

G_y

Figure 2.2 Sobel kernels of the x and y directions.

2.3.3 Morphological Operations

The morphological operation [23] is a topic of mathematical morphology tools for image object extraction. The fundamental of mathematical morphology is based on the set theory. The term morphology refers to the description of the properties of shape and structure of any objects which are represented in sets.

1) Binary Morphology

The operation is applied to a binary image whose white pixels describe a complete morphology of the image. This technique concerns about the object co-ordinates whose value of interested object is 1 while another is 0. The basic operators of the mathematical morphology are erosion, dilation, closing and opening.

1.1) Erosion and Dilation

For dilation, with *A* and *B* are the set in Z^2. The dilation of *A* by *B* denoted as $A \oplus B$ is defined as

$$A \oplus B = \left\{ z \mid \left[(\hat{B})_z \cap A \right] \subseteq A \right\} \tag{4}$$

Set *B* refers to the structure element of the dilation where $\hat{B}$ is the reflected version of B. The operation of $A \oplus B$ is similar to the convolution except the structure element *B* B is reflected instead of flipped. If some elements of $\hat{B}$ are in *A*, the pixel nearby the *A* which in $\hat{B}$ is labeled by 1. The result of dilation is the expansion of *A* by the structure element $\hat{B}$. For erosion, with *A* and *B* are the set in Z^2. The erosion of *A* by *B* denoted as $A \ominus B$ is defined as

$$A \ominus B = \left\{ z \mid B_z \subseteq A \right\} \tag{5}$$

Set *B* refers to the structure element of the erosion. The erosion of *A* by *B* is the set of all points in *z* that *B* contained in *A* with translation of *B* by *z* (B_z). At a certain position every single pixel of structure element overlap with pixel binary image, then element of *A* at the origin of *B* is labeled. If the *A* is smaller than *B*, *A* will disappear. The result of erosion is the object *A* shrinking by the structure element *B*.

1.2) Opening and Closing

Opening and closing are the operation of erosion and dilation. The opening of *A* by structure element *B* denoted by

$$A \circ B = (A \ominus B) \oplus B \tag{6}$$

The closing of *A* by structure element *B* denoted by

$$A \bullet B = (A \oplus B) \ominus B \tag{7}$$

Opening operation generally use for image smoothing, small objects and thin line elimination and gap widening. In contrary, closing operation tends to generate a connection, elongate the long thin line and fill the gap or small hole inside the object

2) Gray Scale Morphology

The morphological operation applied on gray scale image is extended from the binary. The structuring elements (SE) perform the similar function to the binary operation. SE is divided into 2 types, i.e., flat and nonflat. In this study, only flat SE is mentioned since the implementation is simpler. Also, flat SE is symmetry and an origin locates at the center. The operators consist of erosion, dilation, opening and closing as described below

2.1) Erosion and Dilation

The erosion of f by a symmetrical flat SE b at (x, y) is denoted by the minimum value of the intensity in the overlapped region between f and b when the center of b locates at (x, y)

$$[f \ominus b](x, y) = \min_{s,t \in b} \{ f(x+s, y+t) \} \tag{8}$$

On the other hands, dilation of f by a symmetrical flat SE, b at (x, y) is defined as the maximum value of the intensity in the overlapped region between f and $\hat{b}$ when the center of $\hat{b}$ locate at (x, y)

$$[f \oplus b](x, y) = \max_{s,t \in b} \{ f(x-s, y-t) \} \tag{9}$$

where $\hat{b} = (-x, -y)$ is the reflected version of b. The gray-scale erosion with symmetrical flat SE computes the minimum intensity among the coincident regions so the expected result image should be darker. Also, the region of the bright pixel will be decrease depending on the SE size. Likewise, the effect of dilation is opposite to the erosion that the bright region becomes thickened while the dark feature is reduced.

2.2) Opening and Closing

Opening and closing operators of gray scale image are similar to binary implementation. The opening of image *f* by SE *b* can be denoted by

$$f \circ b = (f \ominus b) \oplus b \tag{10}$$

Similarly, the closing of image f by SE b can be denoted by

$$f \bullet b = (f \oplus b) \ominus b \tag{11}$$

Opening operator is generally used to eliminate some small bright objects. However, the larger bright region cannot be removed if the size of SE is not large enough. In contrast, the closing operator is used to remove the dark features whose size related to SE.

2.3) Top-Hat Transform

Top-hat transform is the subtraction of the original image with the opening or closing image. It relies on the fact that gray-scale opening or closing can remove some objects from the image. Subtracting the opened or closed resulting image from original one retain only the objects which have already been removed. The opening top-hat, so-called white top-hat transform, of the image f is defined by

$$T(f) = f - (f \circ b) \tag{12}$$

the opening top-hat transform tends to enhance the object whose intensities are brighter than background. In contrast closing top-hat, so-called black top-hat transform, of the image f is defined by

$$T(f) = f - (f \bullet b) \tag{13}$$

The result of the closing top-hat transform is opposite to the opening top-hat transform that the objects whose intensities are darker than the background will stand out.

Top-hat transform plays a crucial role for non-uniform illumination correction. In this study, we use the top-hat transform for background subtraction, intensity correction and enhancement.

2.3.4 Image Segmentation

1) Watershed Algorithm Based on Distance Map

The watershed algorithm operates on the 3-D topographic surface. Basically, 3-D topography of the gray scale image is generated by the 2-D co-ordinates versus their belonging intensity. Many studies performed the watershed-based segmentation framework on the 3-D topographic surface which generated from binary image by using the distance transform [24, 25]. Given a binary image containing a connected region *R*, the distance transform is the technique for computing the distance between a point in connected component *R* to its boundary points denoted by (*p*, *q*). There are many methods to calculate the distance. Since the WBC candidate has a round shape, using Euclidean is more proper as illustrated in Fig 2.3. The distance of any point (*x*, *y*) in binary region *R* can be defined by

$$D(x,y) = \min_{(x,y)\in R} \sqrt{(p-x)^2 + (q-y)^2} \tag{14}$$

where (*p*, *q*) is a point on the boundary of *R*.

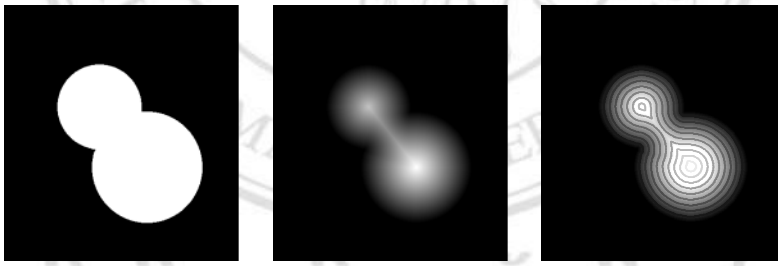

(a) **(b)** **(c)**

Figure 2.3 Euclidean distances transform. (a) Binary image (b) Transformation result (c) Circle contour highlighting.

The watershed algorithm is based on the concept that the gray scale image is visualized by 3-D topography. Each area is detached by the dam. The algorithm will find that dam line. The minimum of each area acts as the spring of the water which was indicated by the black arrow on the Fig.2.4a. The water starts rising through the hole and flooding the topographic area with the uniform rate (Fig.2.4b) until the water of each area is about to merge, the single dam line is generated to protect the merging (Fig.2.4c). Then both areas are detached from each other (Fig.2.4d).

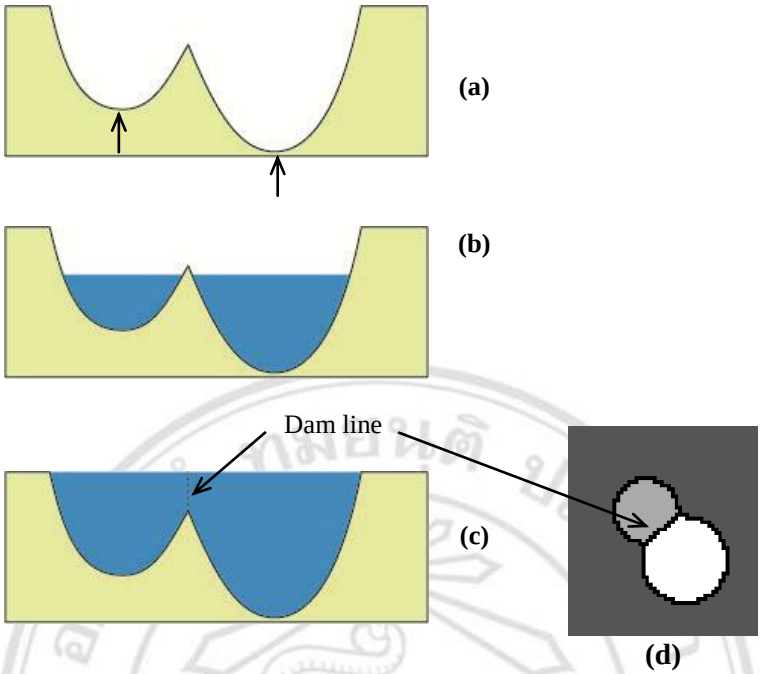

Figure 2.4 Watershed algorithm.

2) Fuzzy C-Means (FCM) Clustering

FCM clustering is an unsupervised clustering method. This process is about to group the element whose individual information is similar while separate the element whose information is different. FCM is called a soft clustering where each element can be the member of every cluster. Membership value of each element depends on the distance to the center of each class. The lower the distance, the higher the membership value to that class is assigned. This technique is very popular and effective in the image processing application especially image segmentation [26-28].

The principle of FCM clustering is briefly described here; Consider a set of data $X = \{\vec{x}_1, \vec{x}_2, ..., \vec{x}_n\}$ where $\vec{x}_k$ is the feature vector. Assuming the fuzzy pseudo-partition of each cluster is $P = \{A_1, A_2, ..., A_c\}$ where c is the number of cluster. The grades of membership of all $\vec{x}_k$ to cluster i are in A_i. The center of c clusters in feature space can be computed by

$$\vec{v}_1 = \frac{\sum_{k=1}^{n} [A_i(\vec{x}_k)]^m \vec{x}_k}{\sum_{k=1}^{n} [A_i(\vec{x}_k)]^m} \tag{15}$$

where $i = 1,2,\ldots,c$ and $m>1$. Then, performance index J_m can be computed by

$$J_m(P) = \sum_{k=1}^{n} \sum_{i=1}^{c} \left[A_i\left(\vec{x}_k\right) \right]^m \left\| \vec{x}_k - \vec{v}_i \right\|^2 \tag{16}$$

The algorithm tried to minimize the value of P that makes $J_m(P)$ decrease in order to reduce the dissimilarity within the class while randomly setting the center of each cluster. The fuzzifier m in which $1 \leq m < \infty$ inferred a decreasing of $J_m(P)$ better than the best hard discrimination [29]. The optimized solution of this problem was published in [30].